

SERS-based detection of 5-S-cysteinyl-dopamine as a novel biomarker of Parkinson's Disease in artificial biofluids

Isidro Badillo-Ramírez^{a*}, Bruno Landeros-Rivera^b, José M. Saniger^c, Jürgen Popp^{d,e} and Dana Cialla-May^{d,e}

^a Center for Intelligent Drug Delivery and Sensing Using Microcontainers and Nanomechanics (IDUN), Department of Health Technology, Technical University of Denmark, Kongens Lyngby 2800, Denmark

^b Facultad de Química, Departamento de Física y Química Teórica, Universidad Nacional Autónoma de México, Circuito exterior S/N, Ciudad Universitaria, 04510, Ciudad de México, Mexico.

^c Instituto de Ciencias Aplicadas y Tecnología, Universidad Nacional Autónoma de México, Circuito exterior S/N, Ciudad Universitaria, 04510, Ciudad de México, Mexico.

^d Friedrich Schiller University Jena, Institute of Physical Chemistry and Abbe Center of Photonics, Helmholtzweg 4, 07743 Jena, Germany

^e Leibniz Institute of Photonic Technology Jena, Member of the Leibniz Research Alliance – Leibniz Health Technologies, Albert-Einstein-Str. 9, 07745 Jena, Germany

*Corresponding author: I-BR (ibara@dtu.dk)

Supplementary Information

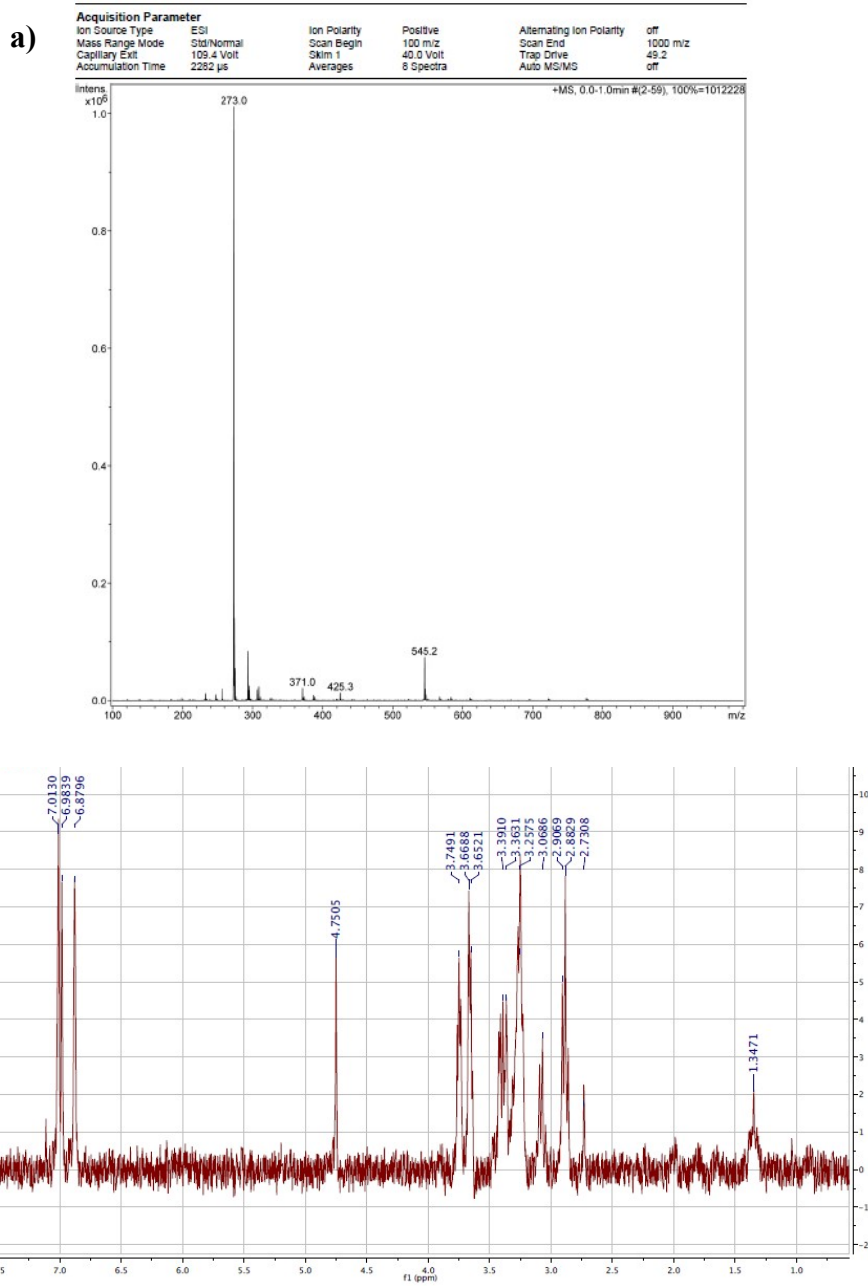


Fig. S1. Spectroscopic characterization of CDA after purification. a) Electrospray ionization mass spectrometry (ESI-MS) analysis; main abundance peak is at 273.0. b) Proton nuclear magnetic resonance (Bruker Avance 300 MHz) of CDA, molecular coupling (chemical shifts) correlated to the reported molecular structure of CDA.

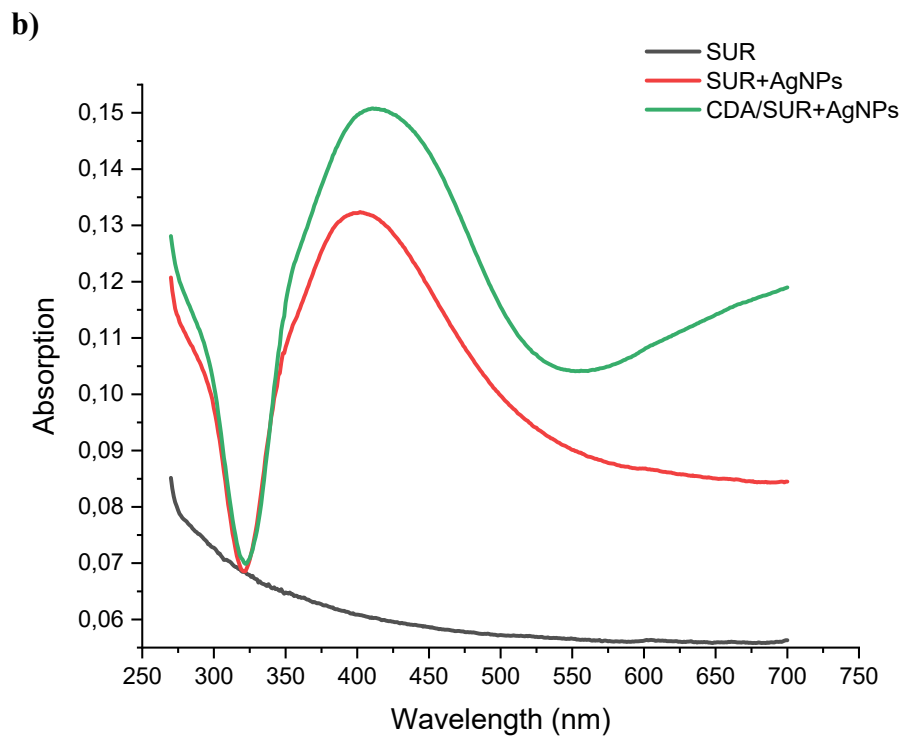
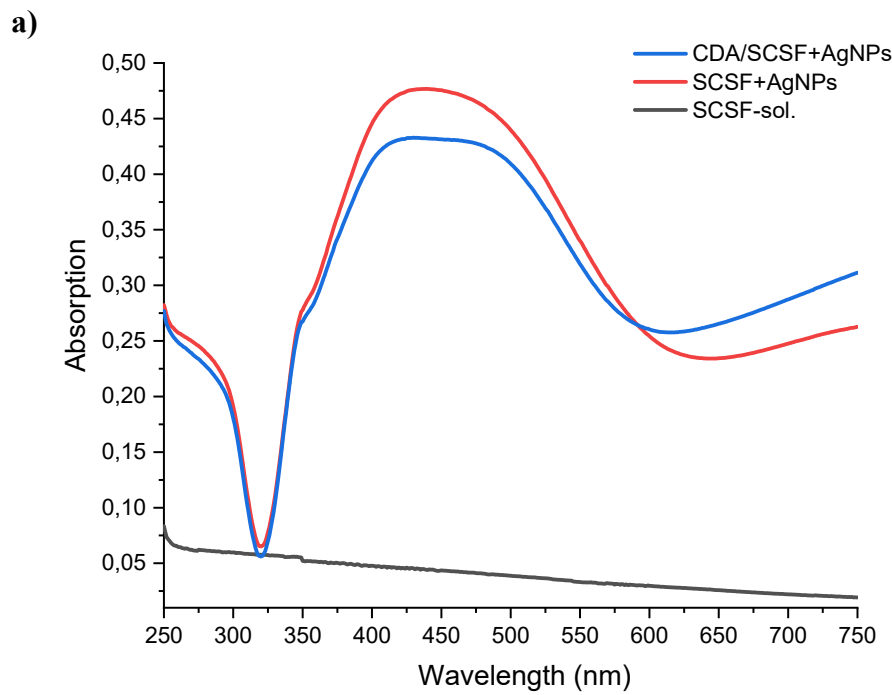


Fig. S2. UV-vis absorption bands of reference solutions of simulated biological fluids and their mixture with colloid nanoparticles: a) SCSF and b) SUR.

Table S1. Calculated Raman, calculated SERS and experimental SERS band assignments of CDA in different media.

Tentative band assignment	Calculated Raman (cm ⁻¹)	Calculated SERS (cm ⁻¹)	SERS CDA/H ₂ O (cm ⁻¹)	SERS CDA/SCSF (cm ⁻¹)	SERS CDA/SUR (cm ⁻¹)
NH ₂ , NH ₃ ⁺ def.	1656	1642	1654	1650	
C=C ring str./ NH ₂ sci./NH ₃ def.	1629	1606	1616	1616	
Arom. ring str./ OH def. (catechol)			1577	1577	1565
C-C (arom.)/ C-O-H in-plane bend.			1546	1542	
C-C ring str./ OH def. (catechol)	1512	1498	1498	1507	1504
Ring def./ C-O-H in-plane def./N-C-H def.	1485	1435	1445	1445	1440
C-C str. (arom.)/C-O-H in-plane bend./COO ⁻ asym str.	1386	1417/1372	1419	1419	1416
CH wag./NH twi./ COO- str./ COH bend.	1323	1327	1330	1330	1339
Ring breathing/CH in-plane rock. (arom.)/ CCH bend.	1305	1309/1282	1267	1271	1270
CH ₂ in-plane bend./ NH ₂ twist.	1251	1255	1226	1230	1228
CH ₂ in-plane bend./C-O-H bend. (catechol)/ CO str.	1212	1201	1199	1199	
C-N str. / S-C-C-N twist./ C-O str.	1152	1165	1139	1144	1143
S-C-C-N tor./ NH ₂ bend.		1084			
C-S-C in-plane bend. (arom.)/ C-S-C-N def. (arom.)	1026				
Urea				1002	
C-N str C-C def. (arom.)/ N-C-H and H-C-H def./ C-OH def. (catecol)			996	996	928
CH in-plane bend./NH ₂ wag./ skeletal C-C str.	891	895		898	
O-H out-of-plane def.		868	870	874	
CH wag. (arom.)/OH rock./ H-N-C in-plane def.	837	832	813		818
COO ⁻ bend./NH ₂ wag./C-C-S def.	801/738		789	789	768
C-S str. /Ring breath due to S/ C-COO ⁻ def.	693	706	664	664	660
S-C ring out-of plane def./ C-S str. /COO- out-of plane def.	639	634/616	616	611	612
C-S-C def./ring out-plane def./ NH ₃ ⁺ rock.	585	562	562	562	570
CCN def./COOH def./ C-S def.					469
Arom. Ring out-of plane def.	414	436	414	414	410

Abbreviations: arom. (aromatic); asym. (asymmetric); bend. (bending); def. (deformation); vibr. (vibration); sym. (symmetric); str. (stretching); twist. (twisting); tors. (torsion); twist. (twisting); wag. (wagging).

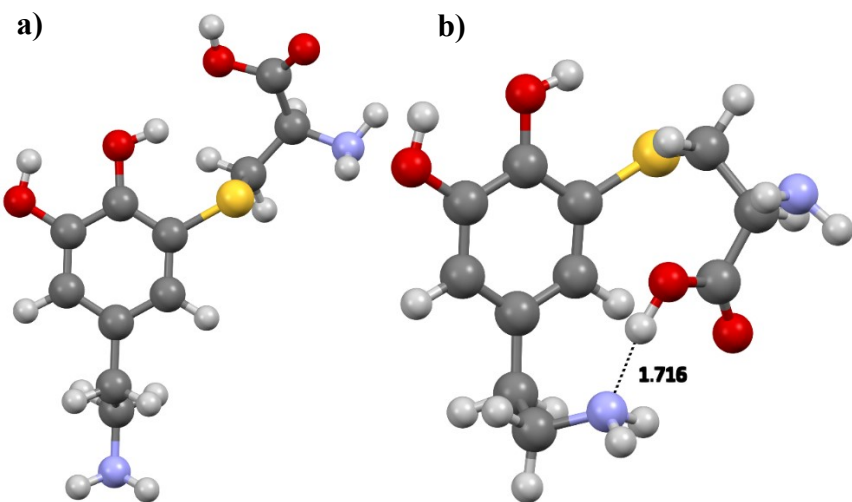


Fig. S3. Calculated CDA molecular configurations: a) open and b) closed. The intramolecular hydrogen bond distance in the closed configuration is 1.716 Å.

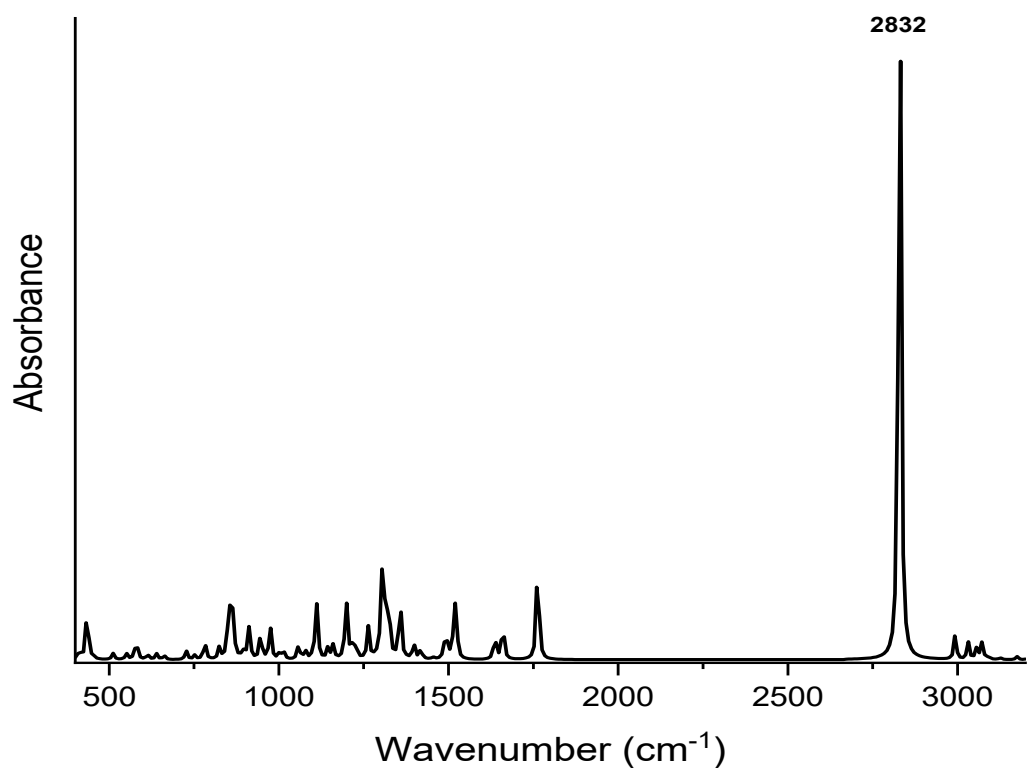


Fig. S4. Calculated FTIR spectrum of CDA on its closed conformation.

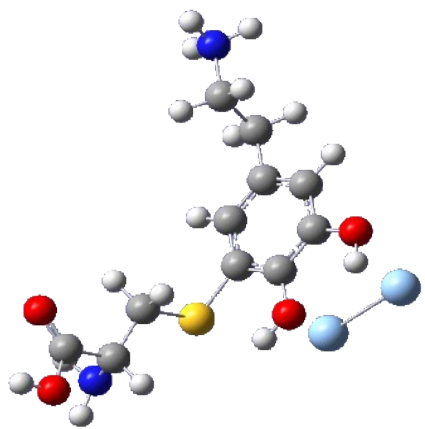


Fig S5.- Simulated CDA open configuration with catechol orientation towards the Ag dimeric atoms.

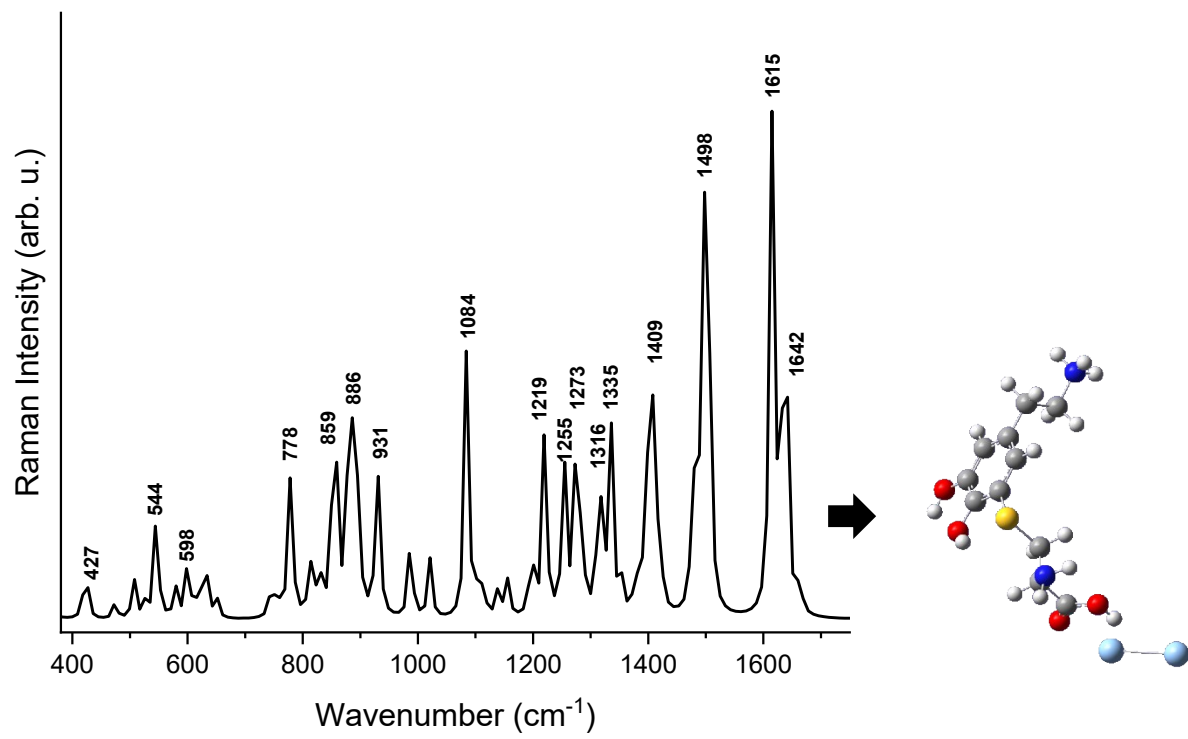


Fig S6.- Calculated SERS spectra of CDA on its open configuration with carboxylic acid orientation towards the Ag dimeric atoms.

Table S2. Values for the electron density (ρ_B), laplacian ($\nabla\rho_B^2$) and electron energy density (H_B) at the bond critical points, in atomic units. The corresponding delocalization indexes (DI) and the classification for each type of interaction are also shown.

Interaction	ρ_B	$\nabla\rho_B^2$	H_B	DI	Classification
Complex I					
H···Ag	0.014508	0.037751	0.000494	0.08	vdW
H···Ag	0.002838	0.005871	0.000237	0.02	vdW
O→Ag	0.029478	0.116765	-0.001645	0.26	Dative
Complex II					
H···Ag	0.005036	0.011180	0.000404	0.03	vdW
H···Ag	0.016298	0.044375	0.000662	0.08	vdW
O→Ag	0.051381	0.246234	-0.003937	0.35	Dative
Complex III					
H···Ag	0.020080	0.046166	-0.000297	0.08	Strong vdW
O···Ag	0.010264	0.033325	0.000964	0.07	vdW
S→Ag	0.056663	0.145587	-0.011001	0.53	Dative